

# **Chemical Preintercalation Synthesis of Versatile Electrode Materials for Electrochemical Energy Storage**

*Ekaterina Pomerantseva*

Department of Materials Science and Engineering, Drexel University, Philadelphia, PA 19104

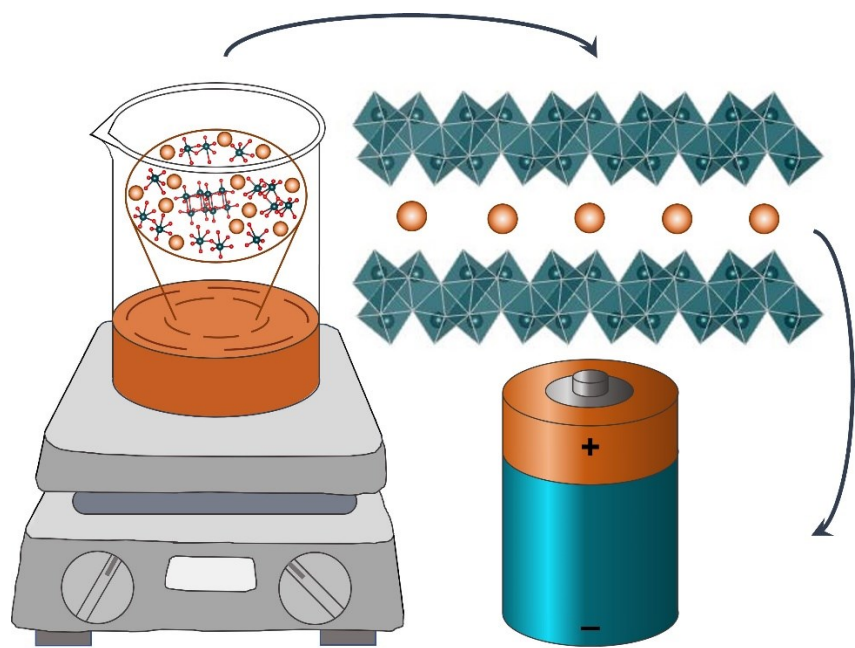
## **CONSPECTUS:**

The widespread use of electrical plants and grids to generate, transmit and deliver power to consumers makes electricity the most convenient form of energy to transport, control and use. Balancing electricity demand with electricity supply requires a mechanism for energy storage, which is enabled by electrical energy storage devices such as batteries and supercapacitors. In addition to the grid-level energy storage, we have all witnessed the quick growth of the number of applications that require autonomous power, illustrated by the Internet of Things, and electrification of transport. Batteries, when developed for targeted applications with specific requirements, require new materials with improved performance enabled by rational design on the atomic level. The material tunability knobs include chemical composition, structure, morphology and heterointerfaces among others. Synthesis methods that would enable control of these parameters while offering versatility and being facile are highly desired.

In this Account, we describe a synthesis strategy for the creation of new intercalation host oxides, hybrid materials, and compounds with oxide/carbon heterointerfaces for use as electrodes in intercalation batteries. We begin by introducing a strategy called the “chemical preintercalation synthesis approach,” and describing processing steps that can be used to tune the material’s chemical composition, structure and morphology. We then show how chemical preintercalation of

inorganic ions can be used to improve ion diffusion and stability of the synthesized materials. We reveal how confined interlayer water can be controlled and how the hydration degree affects electrochemical performance. This is followed by a demonstration of chemical preintercalation of organic molecules leading to unprecedented expansion of the interlayer region up to  $\sim 30$  Å and initial electrochemical characterization of the obtained hybrid materials. We then present evidence that carbonization of the interlayer organic molecules is an efficient synthetic pathway to create oxide/carbon heterointerfaces and improve electronic conductivity of oxides, which leads to improved stability and rate capability during electrochemical cycling. The examples discussed in this Account show that the chemical preintercalation synthesis approach opens pathways for the preparation of materials that have not been synthesized previously, such as new phases, hybrid materials, and 2D heterostructures with advanced functionalities. We demonstrate that chemical preintercalation can be used to effectively tune the chemistry of the confined interlayer region in layered phases and form tight oxide/carbon heterointerfaces enabling control of the materials properties at the atomic level.

## CONSPECTUS GRAPHIC



## Key References

- Clites, M.; Hart, J.L.; Taheri, M.L.; Pomerantseva, E. Chemically Preintercalated Bilayered  $K_xV_2O_5 \cdot nH_2O$  Nanobelts as a High-Performing Cathode Material for K-Ion Batteries. *ACS Energy Lett.* **2018**, *3*, 562-567.<sup>1</sup> *This work provides experimental data and analysis suggesting that high electrochemical performance of chemically pre-potassiated bilayered vanadium oxide could be attributed to the facilitated diffusion of electrochemically cycled  $K^+$  ions through well-defined intercalation sites, formed by chemically preintercalated  $K^+$  ions.*
- Clites, M.; Pomerantseva, E. Bilayered Vanadium Oxides by Chemical Pre-Intercalation of Alkali and Alkali-Earth Ions as Battery Electrodes. *Energy Storage Mater.* **2018**, *11*, 30-37.<sup>2</sup> *This is the first report on chemical preintercalation of alkali and alkaline-earth metal ions into the interlayer region of bilayered vanadium oxide and effect of the nature of chemically preintercalated ion on the structure and electrochemical stability of forming materials.*
- Ridley, P.; Gallano, C.; Andris, R.; Shuck, C.E.; Gogotsi, Y.; Pomerantseva, E. MXene-Derived Bilayered Vanadium Oxides with Enhanced Stability in Li-Ion Batteries. *ACS Appl. Energy Mater.* **2020**, *3*, 10892–10901.<sup>3</sup> *This study for the first time presents synthesis of chemically preintercalated bilayered vanadium oxides (CP-BVOs) with flower-like morphology using two-dimensional (2D) vanadium carbide nanoflakes ( $V_2CT_x$  MXene) as a precursor and reveals morphological stabilization of CP-BVO electrodes in Li-ion cells.*
- Clites, M.; Andris, R.; Cullen, D.A.; More, K.L.; Pomerantseva, E. Improving Electronic Conductivity of Layered Oxides through the Formation of Two-Dimensional Heterointerface for Intercalation Batteries. *ACS Appl. Energy Mater.* **2020**, *3*, 3835-3844.<sup>4</sup>

*This paper demonstrates formation of 2D heterointerface between structural oxide and carbon layers via chemical pre-intercalation of organic molecules followed by carbonization; the enhanced electrochemistry is ascribed to the increased electronic conductivity and improved structural stability enabled by oxide/carbon heterointerface.*

## 1. INTRODUCTION

Chemically preintercalated layered materials have emerged as promising alternatives to classical intercalation battery electrodes.<sup>1-4</sup> Li-ion batteries are currently the most widely used energy storage devices due to the high energy and high power density they exhibit.<sup>5</sup> While it is expected that batteries will mainly use lithium ions at least in the next few years, more abundant and hence less expensive ions, such as sodium, potassium, magnesium and aluminum, attract attention for the development of new energy storage systems.<sup>6,7</sup> However, ions beyond lithium are either larger in size than the lithium ion, or they carry a higher charge, which limits their diffusion in the crystal lattices of electrode materials. Additionally, safety concerns spark interest in developing batteries with aqueous electrolytes. Recent advances with water-in-salt electrolytes (WISE) show that electrochemical water splitting can be suppressed thus expanding a potential window and increasing the energy density of aqueous batteries.<sup>8</sup> These considerations paint a path forward to the production of batteries operating with diverse electrolyte compositions, including both solvents and electrochemically cycled ions. Such technology development poses a need to create new electrode materials that would be compatible with new electrolyte systems and capable of efficiently transferring various types of ions in confined environments. This is particularly important for cathodes, since the cathode is currently a bottle-neck element in commercial batteries, which, due to the limited capacities, does not allow breakthroughs in energy storage technology.

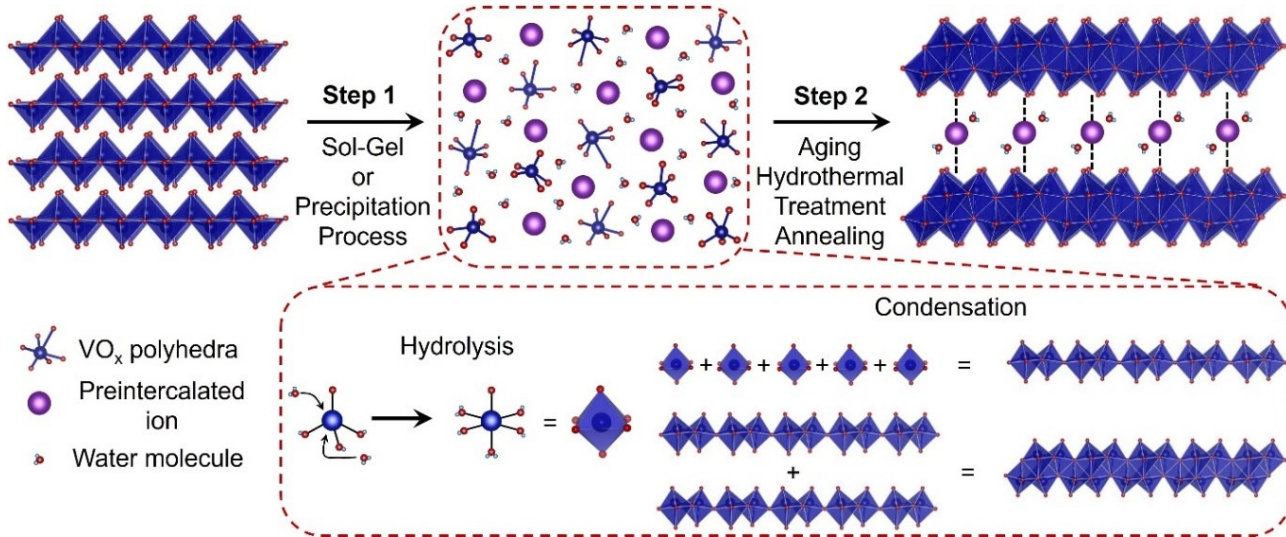
Because of their high potential when interacting with ions from electrolytes, oxides are the most attractive candidates for use as cathodes in batteries. However, in many cases the electronic conductivity of oxides is low, limiting the kinetics and power density of the batteries.<sup>7,9</sup> In commercial batteries, this issue is solved by physically mixing oxides with nanostructured carbons,

serving as conductive additives. But morphological evolution of the electrode during battery operation revealed substantial displacement of the particles leading to the breakage of conductive pathways and loss of performance. In addition, physical mixing with carbon helps to improve only interparticle conductivity, while intraparticle conductivity remains low. Atomic-level nanoscale integration of oxides with carbon with the formation of tight oxide/carbon heterointerfaces is desirable to mitigate this issue.<sup>10</sup> It can be achieved by creating two-dimensional (2D) heterostructures or tightly integrated nanocomposites.

The operation of lithium-ion batteries (LIBs) is based on the process called intercalation.<sup>5, 11</sup> Intercalation is a chemical reaction, generally reversible, that involves the introduction of a guest species into a host structure without a major structural modification of the host. In batteries, the intercalation reaction is an electrochemically driven process in which ions from electrolytes are being inserted into the cathode material structure on discharge, and they are being extracted from the cathode structure and being inserted into the anode structure on charge. In this article, we will be discussing only intercalation-based energy storage devices and therefore we will call them batteries, regardless of the aqueous or non-aqueous nature of the electrolyte, though pseudocapacitors also rely on intercalation processes in addition to surface storage during their operation.

Many transition metal oxides, including vanadium oxide, can be synthesized through low-temperature sol-gel or precipitation processes.<sup>12</sup> One of the synthesis approaches involves dissolution of the metal precursor in aqueous media using hydrogen peroxide. Through the sequence of hydroxylation and condensation reactions, the oxide layers grow from the solution and assemble into a structure with lamellar ordering with interlayer water molecules. We modified this process by introducing foreign species, such as inorganic or organic ions, which were added

into reaction mixture during solution stage in the form of water-soluble salts (**Figure 1**). The cations from these species are trapped between the growing oxide layers, producing a wide family of new chemically preintercalated layered materials.<sup>2, 13</sup> In addition, we demonstrated that the precipitate obtained through the sol-gel step can be further processed using aging, hydrothermal treatment and annealing (**Figure 1**), providing another level of control of the chemical composition and structure of the synthesized materials.<sup>14, 15</sup> Because the layered framework of the oxide phase is preserved, and only interlayer spacing and chemical composition of the interlayer region are affected, we called this synthesis method, schematically shown in **Figure 1**, *a chemical pre-intercalation synthesis approach*. This name indicates that expansion and contraction of the layers, typical for layered phases in intercalation reactions, occur chemically during material formation, rather than through a post-synthesis interlayer exchange process or electrochemically driven ion insertion.



This Account highlights the promise of the chemical preintercalation synthesis approach for the creation of new layered phases with directional and controllable ion transport, inorganic/organic hybrid materials and 2D heterostructures with tight oxide/carbon heterointerfaces. We review the available reports on chemical pre-intercalation synthesis of electrode materials with the focus on atomic-level control leading to enhanced transport of ions and electrons leading to superior electrochemical performance in energy storage systems. We then outline the future steps, enabled by chemical pre-intercalation, to create new electrodes that could greatly expand current energy storage technologies.

## 2. CHEMICAL PREINTERCALATION OF INORGANIC IONS

Chemical preintercalation of inorganic ions has been focused on developing a synthetic ability to incorporate metal ions with low atomic mass to maintain the light molecular weight of the produced electrode material leading to the light batteries and high gravimetrically scaled battery performance characteristics. In the case of inorganic ions, we realized that the chemical preintercalation synthesis method can be used to investigate two distinct directions. First, one can chemically preintercalate electrochemically active ions (*for example, Na<sup>+</sup> ions in the case of Na-ion batteries*) with the aim to create positions in the structure of the host favored by these ions and thus improve ion diffusion (**Figure 2a**). And second, one can chemically preintercalate electrochemically inactive species (*for example, Mg<sup>2+</sup> ions in the case of Li-ion batteries*) with the aim to improve structural and electrochemical stability of electrode materials. This second direction is also called the pillarizing approach (**Figure 2b**).

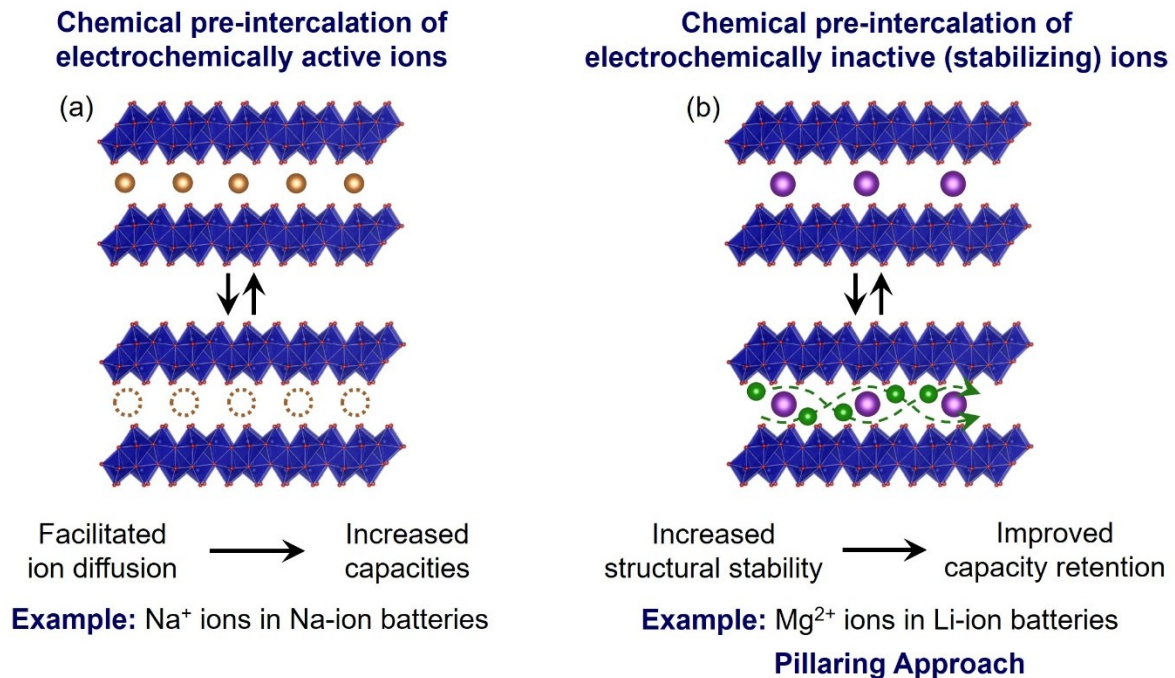


**Figure 2.** Schematic illustration of (a) diffusion and (b) stabilization improvements in battery electrode materials that can be achieved via chemical preintercalation of inorganic ions.

Chemical preintercalation with inorganic ions was pioneered by Liqiang Mai et al. with the first synthesized material being lithiated  $\text{MoO}_3$  nanobelts.<sup>16</sup> Chemical lithiation was achieved by mixing  $\alpha\text{-MoO}_3$  nanobelts with  $\text{LiCl}$  solution, which was stirred for two days and then hydrothermally treated at  $180^\circ\text{C}$  for 24 h. The lithiated  $\text{MoO}_3$  nanobelts demonstrated improved cycling stability, with a capacity retention of 92% after 15 cycles, as compared to the non-lithiated  $\text{MoO}_3$  nanobelts which retained only 60% of capacity in non-aqueous Li-ion cells. The synthesis method was later expanded to obtain Na-preintercalated  $\text{MoO}_3$ .<sup>17</sup> Compared to pristine  $\text{MoO}_3$ , the presodiated  $\text{MoO}_3$  nanobelts showed significant improvements in cycling stability and rate capability in non-aqueous Li-ion cells. Using *in situ* XRD analyses combined with electrochemical tests, it was found that the  $\text{Na}^+$  ions between the Mo-O layers inhibit the irreversible phase

transformation and stabilize the layered  $\text{MoO}_3$  structure leading to the improved electrochemical stability.

One of the attractive hosts for chemically preintercalated species is bilayered vanadium oxide (BVO) or  $\delta\text{-V}_2\text{O}_5\cdot n\text{H}_2\text{O}$ .<sup>18, 19</sup> BVO exhibits intercalation of lithium ions at relatively high voltages making it an attractive candidate for cathode applications. Vanadium is a transition metal ion that is present in this material in the oxidation state of +5, and it can undergo several reduction steps. The layered structure of BVO is characterized by an expanded interlayer region with an interlayer distance of 11.5 Å, which is stabilized by water molecules.<sup>18</sup> Additionally, materials such as BVO are attractive for applications as cathodes in not only Li-ion but also beyond Li-ion batteries, since the expanded interlayer region can accommodate larger electrochemically cycled ions, such as sodium and potassium, and there could be a possibility of shielding a larger charge in the case of magnesium and aluminum ions due to the presence of water in the interlayer region.<sup>19</sup> In aqueous energy storage systems, the facilitated diffusion of ions removed from water-based electrolytes can be enabled by confined interlayer water in BVO structure.<sup>20</sup> Therefore, hydrated layered compounds, such as BVO, are attractive candidates to be used as electrodes in both aqueous and non-aqueous energy storage cells.

### **Diffusion**

Preintercalation of vanadium oxide with electrochemically active ions has been shown to lead to advanced electrochemical performance in non-aqueous Mg-ion batteries<sup>21</sup> and aqueous Zn-ion batteries.<sup>22</sup> Both cases demonstrated not only high initial capacity, but also improved capacity retention and rate capability. The improved electrochemical performance is attributed to the facilitated diffusion of the electrochemically cycled ions in the structure of the preintercalated host material.

Because of the large size and mass of potassium ions hindering their diffusion, we selected K-preintercalated BVO in non-aqueous K-ion batteries as a system to investigate the effect of chemically preintercalated electrochemically cycled ions on charge storage properties.<sup>1</sup>  $\delta$ -K<sub>0.42</sub>V<sub>2</sub>O<sub>5</sub>·0.25H<sub>2</sub>O with the interlayer spacing of 9.65 Å (**Figure 3**) showed the initial discharge capacity of 226 mAh/g at a current rate of C/15 and capacity retention of 74% after 50 discharge/charge cycles. When the current rate was increased from C/15 to 1C, 58% capacity retention was observed (**Figure 3**). The mechanism of charge storage was determined to be dominated by diffusion-controlled intercalation.<sup>1</sup> We attributed the promising charge storage properties of  $\delta$ -K<sub>0.42</sub>V<sub>2</sub>O<sub>5</sub>·0.25H<sub>2</sub>O electrodes to the facilitated diffusion of electrochemically cycled K<sup>+</sup> ions through well-defined intercalation sites, formed by chemically preintercalated K<sup>+</sup> ions.

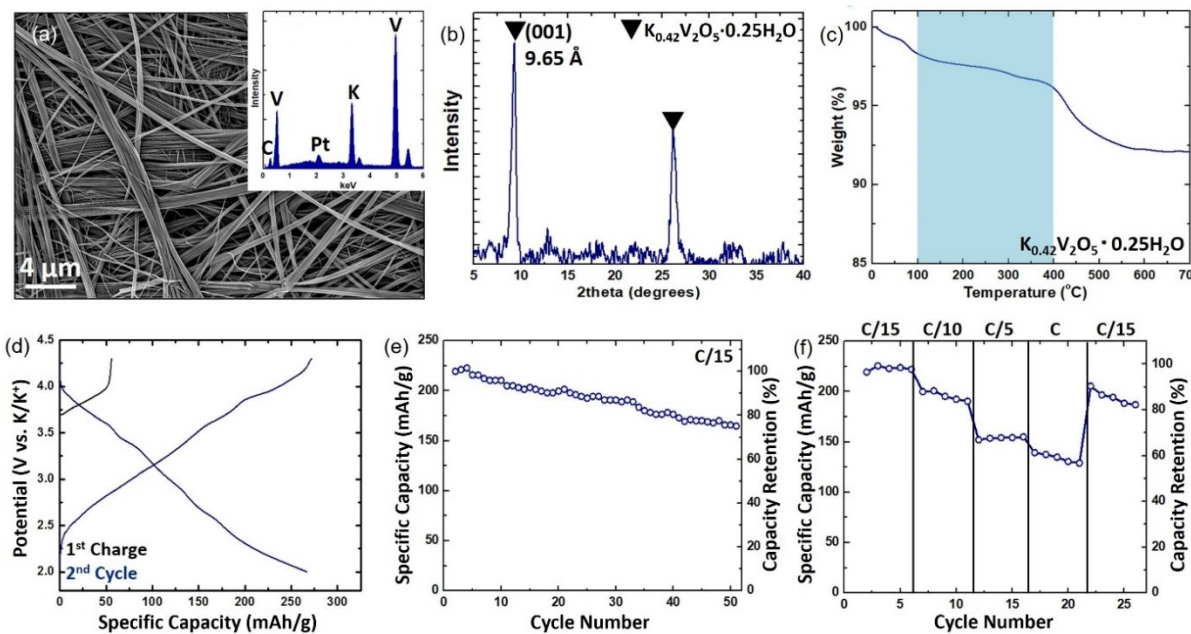


**Figure 3.** Chemical preintercalation of K<sup>+</sup> ions for non-aqueous K-ion batteries. (a) SEM image (the inset shows an EDX spectrum), (b) XRD pattern, and (c) TGA weight loss curve of  $\delta$ -K<sub>0.42</sub>V<sub>2</sub>O<sub>5</sub>·0.25H<sub>2</sub>O. (d–f) Electrochemical cycling of the  $\delta$ -K<sub>0.42</sub>V<sub>2</sub>O<sub>5</sub>·0.25H<sub>2</sub>O electrodes in non-aqueous K-ion cells. Adapted with permission from ref. 1. Copyright 2018 American Chemical Society.

Interestingly, our comparison of three alkali ion systems (Li-preintcalated BVO in Li-ion cells, Na-preintercalated BVO in Na-ion cells, and K-preintercalated BVO in K-ion cells) revealed that in all three cases high initial capacities are exhibited by BVO preintercalated with alkali ions.<sup>23</sup> The mechanism of charge storage was investigated using a method based on analysis of the cyclic voltammogram sweep rate dependence.<sup>24</sup> We found that as the size of the electrochemically cycled ion increases, and the interlayer spacing decreases at the same time, the fraction of the diffusion limited capacity increases. This finding confirms that chemically preintercalating electrochemically cycling ions creates specific crystallographic sites in the interlayer region of the material, which favor accommodation of these ions. As a result, intercalation and diffusion of these ions during electrochemical cycling are facilitated, leading to high performance of the materials. At the same time, high capacities decrease during cycling, raising a question of how this initial high performance can be stabilized.

### **Pillaring**

Pillaring of the BVO with iron,<sup>25</sup> manganese and nickel<sup>26</sup> showed improvement in electrochemical stability of the ion-stabilized materials compared to the BVO containing only water in the interlayer region. It suggests that chemically introduced electrochemically inactive ions form additional bonds with vanadium-oxygen layers, thus suppressing their expansion and contraction, also known as the lattice breathing effect, during electrochemical cycling.

We tested the same approach was tested in Li-ion batteries by systematically inserting alkali (lithium, sodium and potassium) and alkaline-earth (magnesium and calcium) ions into the BVO structure via our developed chemical pre-intercalation synthesis route based on H<sub>2</sub>O<sub>2</sub>-initiated reaction in the presence of chlorides of aforementioned cations.<sup>2</sup> With an  $\alpha$ -V<sub>2</sub>O<sub>5</sub> precursor, all materials demonstrated nanobelt morphologies, only in case of the Ca-preintercalated phase the

nanobelts were not as well-formed as for other materials (**Figure 4a**). Analysis of the XRD patterns revealed that the interlayer spacing can be tuned between 9.6 and 13.4 Å by changing the nature of the preintercalated ions (**Figure 4b**). Moreover, it was found that the interlayer spacing increases with the increase in the size of the hydrated chemically preintercalated ions, suggesting the ions reside in the interlayer region together with their hydration shell.

The pillar effect was investigated by cycling  $\delta\text{-M}_x\text{V}_2\text{O}_5\cdot n\text{H}_2\text{O}$  ( $\text{M} = \text{Li, Na, K, Mg, Ca}$ ) electrodes in Li-ion cells, where the Li-preintercalated phase served as a reference material (**Figure 4c, 4d**). Extended cycling revealed that  $\delta\text{-Mg}_x\text{V}_2\text{O}_5\cdot n\text{H}_2\text{O}$  with the largest interlayer spacing showed the highest capacity retention and rate capability. More interestingly, we found that the cyclability and rate performance of chemically pre-intercalated BVOs in Li-ion cells improved with increasing interlayer spacing.<sup>2</sup> This finding was attributed to a more facile diffusion of small lithium ions in wider 2D diffusion channels. Additionally, it is believed that chemically preintercalated ions introduce ionic bonding between the layers of the host oxide phases thus enabling improved structural stability. Interestingly, it was shown that capacity fading of BVO electrodes in part is caused by the loss of lamellar ordering of the V-O layers during multiple intercalation/extraction cycles.<sup>27</sup> Therefore, enabling improved structural stability via chemical preintercalation of ions is an efficient strategy to achieve enhanced electrochemical stability during battery operation.

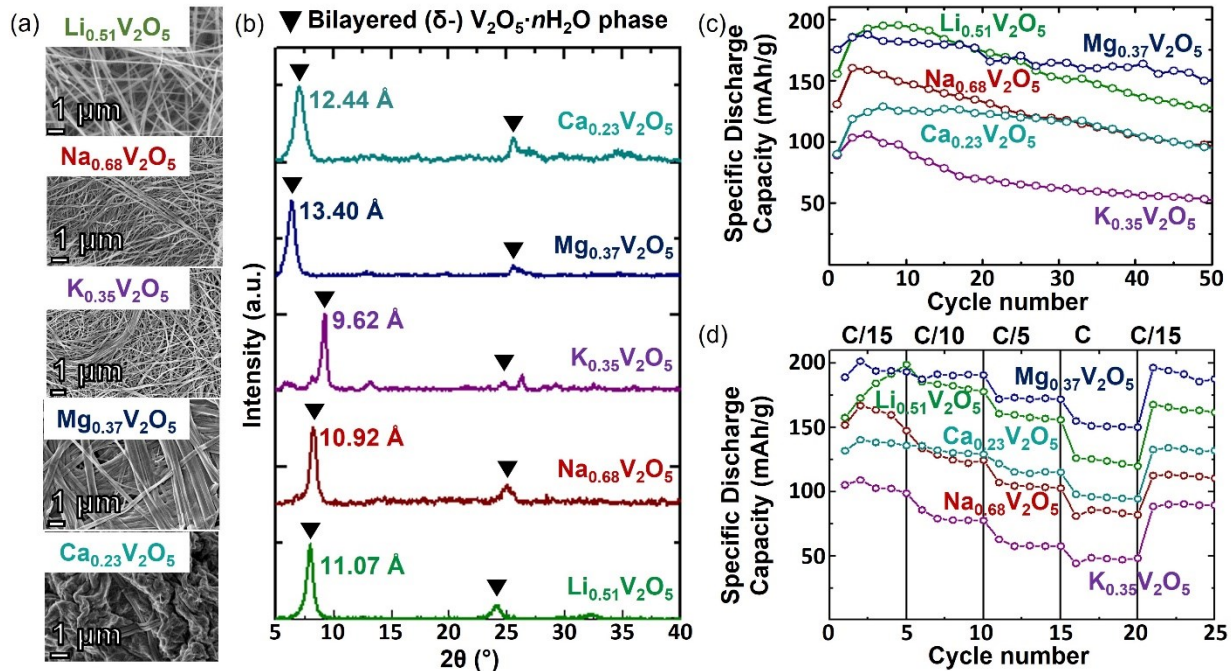


**Figure 4.** Ion-stabilized  $\delta\text{-M}_x\text{V}_2\text{O}_5\cdot n\text{H}_2\text{O}$  ( $\text{M} = \text{Li, Na, K, Mg, Ca}$ ) synthesized via chemical preintercalation synthesis: (a) SEM images and (b) XRD patterns. (c – d) Electrochemical cycling of the  $\delta\text{-M}_x\text{V}_2\text{O}_5\cdot n\text{H}_2\text{O}$  electrodes in non-aqueous Li-ion cells: (c) Cycling performance at a current density of 20 mA/g. (d) Rate performance at the current rates shown in the figure. Adapted with permission from ref. 2. Copyright 2018 Elsevier.

While ease of synthesis makes BVO an excellent material for demonstrating the versatility of the chemical preintercalation approach, other oxides have been successfully synthesized using similar processes. Chemically pre-intercalated molybdenum,<sup>16, 17</sup> titanium,<sup>28</sup> manganese<sup>29, 30</sup> and tungsten<sup>31</sup> oxides have been reported, but they have not yet been as extensively studied for energy storage applications as BVO polymorphs. The chemical versatility of the synthesis approach offers an opportunity to discover never previously synthesized layered materials and open their electrochemical charge storage properties for study.

## Water

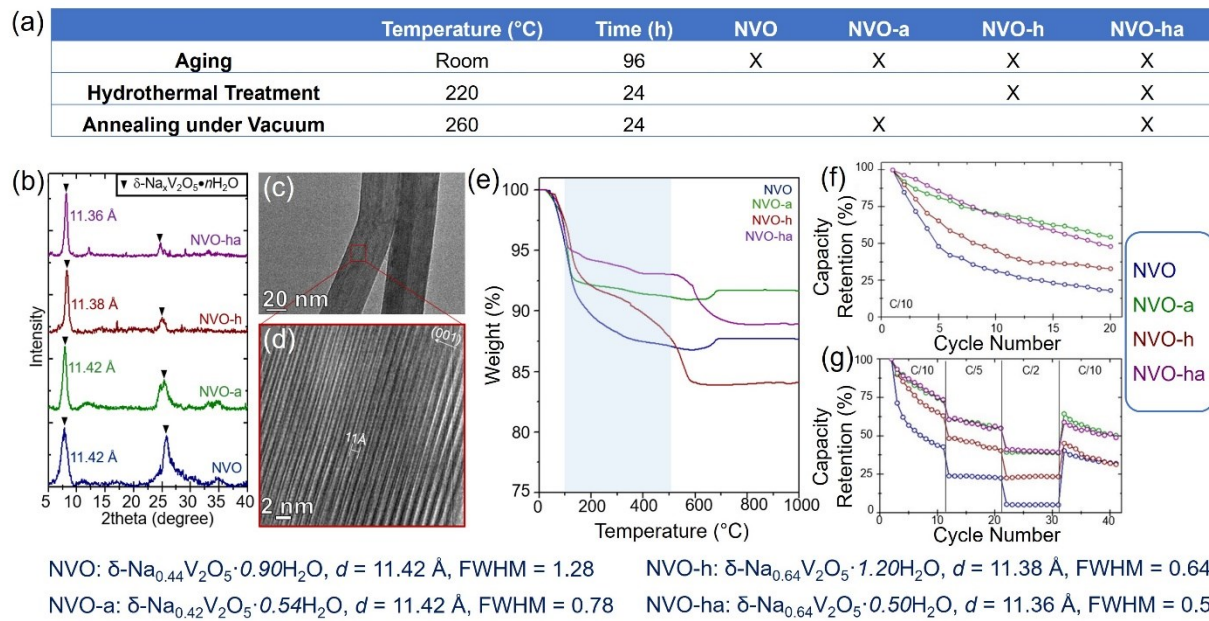


**Figure 5.** Control of the hydration degree leading to the improved electrochemical stability of the  $\delta\text{-Na}_x\text{V}_2\text{O}_5\cdot n\text{H}_2\text{O}$  electrodes in non-aqueous Na-ion cells. (a) Synthesis conditions, (b) XRD patterns and (e) TGA weight loss curves of the NVO, NVO-a, NVO-h and NVO-ha materials. (c) Low-magnification TEM and (d) HRTEM images of the NVO-h nanobelt. (f – g) Electrochemical cycling: (f) cycling performance at a current rate of C/10 and (g) rate performance at the current rates shown in the figure. Adapted with permission from ref. 15. Copyright 2020 American Chemical Society.

While the ion-pillaring approach proved to be an efficient and tunable way to control electrochemical stability, it is important to remember that the interlayer region of chemically preintercalated BVOs also contains water molecules. An interesting study of the confined water in the BVO structure showed that it plays a dual role.<sup>32</sup> First, interlayer water stabilizes expanded interlayer spacing. But at the same time this water can react with electrochemically cycled lithium ions forming lithium hydroxide, a poorly reversible process leading to the capacity fading over cycling.<sup>32</sup> Additionally, loosely bound structural water molecules can dissolve in electrolyte during cycling leading to electrolyte decomposition and a possible interaction with a metallic anode material and the formation of an insulating oxide/hydroxide layer on the anode surface. Therefore,

the water molecules that enable large space for ions intercalation needed to achieve high capacity also cause deterioration of material performance in non-aqueous cells.

Understanding the important role of water in the BVO structure, we attempted to control its amount in the interlayer region by low-temperature vacuum annealing.<sup>15</sup> By carefully selecting the temperature of the annealing, it is possible to minimize the amount of stabilizing water molecules in the interlayer region of BVO without phase transformation. Annealing at 260°C under vacuum (**Figure 5a**) led to enhanced electrochemical stability of  $\delta\text{-Na}_x\text{V}_2\text{O}_5\cdot n\text{H}_2\text{O}$  nanobelts cycled in non-aqueous Na-ion cells.<sup>15</sup> We demonstrated that using low-temperature vacuum annealing, the interlayer water content can be varied in the  $0.50 \leq n \leq 1.20$  range without a significant change in the interlayer spacing (**Figure 5b-e**). The improved capacity retention (**Figure 5f, 5g**) exhibited by low-temperature vacuum annealed  $\delta\text{-Na}_x\text{V}_2\text{O}_5\cdot n\text{H}_2\text{O}$  nanobelts was attributed to the partial removal of the structural water from the interlayer region, formation of additional bonds within the V-O bilayers, and increased stacking order of V-O bilayers.<sup>15</sup> Alternatively, confined water molecules can facilitate charge storage properties in aqueous energy storage systems<sup>20</sup> as demonstrated for tungsten,<sup>33</sup> vanadium<sup>34</sup> and manganese<sup>35</sup> oxides. Therefore, low-temperature vacuum annealing can be used as an efficient strategy to control interlayer water and electrochemical charge storage properties of hydrated transition metal compounds.

## **Precursor**

Another tuning knob that can be used in chemical preintercalation synthesis to achieve improvements in electrochemical charge storage of the synthesized materials is the transition metal oxide precursor. Most BVOs discussed so far have been prepared using a sol-gel reaction between the orthorhombic  $\alpha$ -V<sub>2</sub>O<sub>5</sub> and hydrogen peroxide. Alternative 2D precursors can be found in a diverse family of 2D transition metal carbides, known as MXenes.<sup>36</sup> For example, the reaction between Ti<sub>3</sub>C<sub>2</sub>T<sub>x</sub> MXene and H<sub>2</sub>O<sub>2</sub>, carried out in alkaline solutions (NaOH or KOH), produced ultrathin nanoribbons of layered sodium and potassium titanates.<sup>37</sup> MXenes were also used for the fabrication of 2D MOF sheets and thin films by solvothermally treating V<sub>2</sub>CT<sub>x</sub> and meso-tetra(4-carboxyl-phenyl) porphyrin ligands.<sup>38</sup>

Our experiments with the goal to achieve reorganization of the V<sub>2</sub>CT<sub>x</sub> framework via anionic sublattice modification in the presence of alkali and alkaline-earth ions led to the formation of  $\delta$ -M<sub>x</sub>V<sub>2</sub>O<sub>5</sub>·nH<sub>2</sub>O (M = Li, Na, K, Mg, Ca).<sup>3</sup> We conducted the transformation in a two-step process with the H<sub>2</sub>O<sub>2</sub>-induced reaction followed by hydrothermal treatment. The transformation was accompanied by chemical preintercalation of alkali and alkaline-earth ions via the addition of inorganic chlorides into the reaction mixture, leading to the formation of layered polymorphs with tunable d-spacings in the range between 9.8 and 13.7 Å. The absence of carbon D and G spectral bands in Raman spectra indicated an absence of any bonded or disordered carbon.<sup>3</sup> A possible mechanism of transformation involves formation of carbon-based gaseous species emitted from the reaction vessel, which is consistent with the observed gas evolution during synthesis.

Strikingly, SEM images revealed that by using MXene precursor we synthesized all five chemically preintercalated phases as 2D sheets (**Figure 6a-j**), which has never been reported for BVOs synthesized from  $\alpha$ -V<sub>2</sub>O<sub>5</sub> precursor.<sup>3</sup> Li-preintercalated material formed flexible nanoflakes

stacked into a film-like architecture with some pores between the flakes (**Figure 6a, 6b**). Na-, K-, Mg- and Ca-preintercalated  $\delta$ - $\text{V}_2\text{O}_5 \cdot n\text{H}_2\text{O}$  phases showed a flower-like morphology comprised of 2D nanoplatelets growing outward from the center of the flower (**Figure 6c-j**). In case of Na- and K-containing materials, the nanoplatelets are mostly straight, while nanoflakes of Mg- and Ca-preintercalated phases twist and form more intricate agglomerates.

We selected Li- and Mg-preintercalated MXene-derived BVOs for detailed electrochemical investigation in Li-ion cells (**Figure 6k-p**), as these two materials showed the best performance in case of our synthesis based on  $\alpha$ - $\text{V}_2\text{O}_5$  precursor.<sup>2</sup> After 50 cycles at a current rate of C/3, the Li-preintercalated electrode demonstrated a specific discharge capacity of  $193 \text{ mAh} \cdot \text{g}^{-1}$  with capacity retention of 90%, and the Mg-preintercalated electrode showed a specific discharge capacity of  $184 \text{ mAh} \cdot \text{g}^{-1}$  with a capacity retention of 94%.<sup>3</sup> Interestingly, the best-performing BVO synthesized from  $\alpha$ - $\text{V}_2\text{O}_5$  showed a capacity retention of only 81.8% after cycling for 50 cycles at a current density of  $20 \text{ mA} \cdot \text{g}^{-1}$ .<sup>2</sup> Impressively,  $\text{V}_2\text{CT}_x$ -derived  $\delta$ - $\text{Li}_x\text{V}_2\text{O}_5 \cdot n\text{H}_2\text{O}$  and  $\delta$ - $\text{Mg}_x\text{V}_2\text{O}_5 \cdot n\text{H}_2\text{O}$  electrodes demonstrated exceptional tolerance to high current rates and specific discharge capacities of  $130 \text{ mAh} \cdot \text{g}^{-1}$  and  $146 \text{ mAh} \cdot \text{g}^{-1}$  at a current rate of 5C, respectively.<sup>3</sup> We believe that higher discharge capacity at the highest current rate of Mg-preintercalated electrodes was caused by the elaborate flower-like surface morphology of the Mg-preintercalated phase, which enables higher contact area with the electrolyte compared to the stacked particles of Li-preintercalated phase.<sup>3</sup> We attributed the advanced electrochemical properties to 2D morphology of MXene-derived BVOs combined with the structure and composition of the synthesized materials.

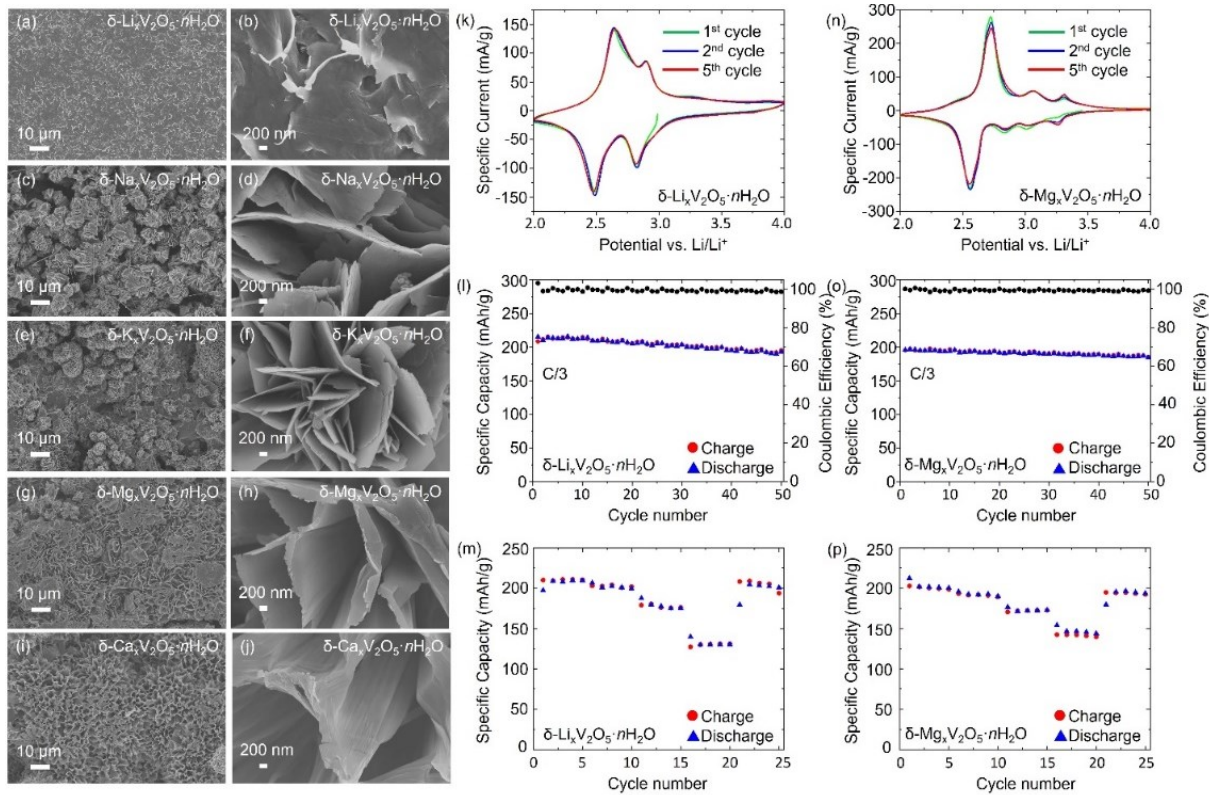


**Figure 6.** MXene-derived  $\delta\text{-M}_x\text{V}_2\text{O}_5\cdot n\text{H}_2\text{O}$  ( $\text{M} = \text{Li, Na, K, Mg, Ca}$ ). (a – j) SEM images of the individual materials labeled in the figure. (k – p) Electrochemical performance of (k – m)  $\delta\text{-Li}_x\text{V}_2\text{O}_5\cdot n\text{H}_2\text{O}$  and (n – p)  $\delta\text{-M}_x\text{V}_2\text{O}_5\cdot n\text{H}_2\text{O}$  electrodes in non-aqueous Li-ion cells. Adapted with permission from ref. 3. Copyright 2020 American Chemical Society.

### 3. CHEMICAL PREINTERCALATION OF ORGANIC IONS

#### Hybrid Phases

Inspired by our finding that Mg-preintercalated BVO, with the largest interlayer distance of all phases synthesized with inorganic ions, showed the highest specific capacity, cyclability and rate capability, we turned our heads into exploring the possibilities to further increase the interlayer spacing. We realized that interlayer region can be expanded beyond the limits achievable via chemical preintercalation of inorganic ions by utilizing large organic molecular ions. Hybrid  $\text{V}_2\text{O}_5$ /organic materials have been synthesized following two synthesis techniques: (1) interaction between  $\text{V}_2\text{O}_5$  xerogel with organic species dissolved in liquid media, often water; (2)

hydrothermal treatment of  $\alpha$ -V<sub>2</sub>O<sub>5</sub> in the presence of organic species. For example, simultaneous intercalation and polymerization of conductive polymers, such as polyaniline and polythiophene, was reported.<sup>39</sup> Other reports showed insertion of metal coordination complexes<sup>40</sup> and polyelectrolytes.<sup>41</sup> It is recognized that due to the negative charge of vanadium-oxygen layers, insertion of cationic species is most efficient. While synthesis and structure of these V<sub>2</sub>O<sub>5</sub>/organic hybrids is described in detail, their charge storage properties were not explored.

In the process of selecting the appropriate organic molecules to be compatible with our H<sub>2</sub>O<sub>2</sub>-initiated aqueous synthesis route, we came up with the following criteria. The organic molecules must be soluble in water, they should form positively charged species, and they should have variable size to observe tunability of interlayer region. For these reasons, we selected several linear organic molecules, decyltrimethylammonia (DTA), decamethonia (DMO) and cetyltrimethylammonia (CTA), have been selected in the form of respective bromides (**Figure 7a**). We found that the structure of the hybrid products depends on the ratio of vanadium oxide and organic molecule precursor. At low organic molecule concentration in the sol-gel synthesis step, regardless of the nature and length of organic species, the interlayer spacing in the produced hybrid materials was around 12.5-12.7 Å (**Figure 7b**). However, when the concentration of organic molecules was increased, DTA-, DMO- and CTA-preintercalated BVOs exhibited interlayer spacing that increased with increase of the length of chemically preintercalated linear organic molecule (**Figure 7b, 7c**). The largest interlayer spacing of about 30 Å was observed for the CTA-preintercalated BVO (**Figure 7b, 7d**), which was confirmed by both XRD characterization and TEM imaging (**Figure 7e**). These results suggest that depending on the concentration of organic molecules in synthesis, they can adopt different orientations in the interlayer region (**Figure 7c**).

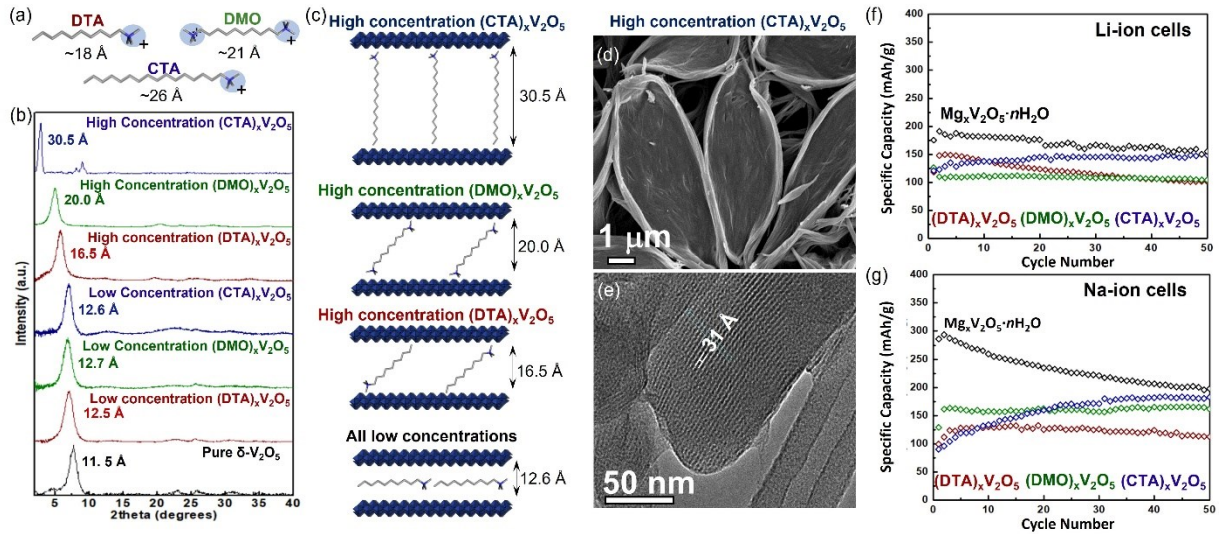


**Figure 7.** Chemical preintercalation of (a) decyltrimethylammonia (DTA), decamethonia (DMO) and cetyltrimethylammonia (CTA) linear organic ion into the interlayer region of BVO. (b) XRD patterns of the samples with high and low organic ion precursor concentrations and non-preintercalated  $\delta$ -V<sub>2</sub>O<sub>5</sub>·nH<sub>2</sub>O. (c) Schematic illustration of the possible orientation of linear organic ions in the interlayer region. (d) SEM and (e) HRTEM images of  $\delta$ -(CTA)<sub>x</sub>V<sub>2</sub>O<sub>5</sub>-sample obtained with high organic precursor concentration. (f – g) Extended cycling of all preintercalated samples synthesized with high organic precursor concentrations in (f) Li-ion and (g) Na-ion non-aqueous cells.  $\delta$ -Mg<sub>x</sub>V<sub>2</sub>O<sub>5</sub>·nH<sub>2</sub>O electrodes were used as a reference. Adapted with permission from ref. 13. Copyright 2018 SPIE – the international society for optics and photonics.

It is likely that at low concentrations linear organic molecules reside in the interlayer region with their chains almost parallel to the vanadium oxide layers. While at higher concentration, linear organic molecules can orient themselves at an angle possibly up to 90°, corresponding the orientation perpendicular to the vanadium oxide layers.

We compared the extended cycling performance of all three hybrid materials in Li-ion and Na-ion cells with the performance of Mg-preintercalated BVO (Figure 7f, 7g). While the initial capacities were lower for all organic-preintercalated phases compared to the reference, some of them demonstrated better capacity retention. Most interestingly, CTA-preintercalated material showed increased capacity over cycling. For this sample, the capacity of 150 mAh/g was measured at cycle

50, similar to the 50<sup>th</sup> cycle capacity of Mg-preintercalated BVO. In Na-ion cells, CTA-containing electrode material again demonstrated activation-like behavior with capacity increasing over cycling. For Na-ion cells, the first cycle capacity was slightly lower than in the following cycles for all three phases. Such electrochemical behavior could indicate evolution and re-arrangement of the interlayer species during cycling that would enable more space for electrochemically cycled Li<sup>+</sup> ions.

### **Oxide/Carbon Heterointerface**

Many 2D materials, such as transition metal dichalcogenides, MXenes, layered oxides and all kinds of graphene-based materials, have been reported as potential electrodes for energy storage.<sup>7</sup> Despite high electrochemical activity, individual layered materials have certain limitations, which can be overcome by combining them by alternating layers of different materials and creating a heterointerface.<sup>10</sup> For example, a major limitation of layered oxides, their poor electronic conductivity, can be mitigated by arranging layers in such a way that oxide layers will alternate with layers of conductive material, such as graphene or MXene. In such materials, often called 2D heterostructures, electrons are transported through the electrically conductive layer and ions move through open 2D diffusion channels.<sup>42</sup>

Assembly can be controlled via a bottom-up approach, in which a 2D heterostructure is grown from the solution. One of the existing reports revealed a reaction between antimony sulfide, sodium molybdate, thiourea and glucose to produce a MoS<sub>2</sub>/C heterostructure with high performance in Na-ion batteries.<sup>43</sup> Enhanced rate performance of the heterostructure compared to that of pure MoS<sub>2</sub> was attributed to the intimate contact at the heterointerface enhancing transport of electrons and Na<sup>+</sup> ions. The bottom-up strategy to synthesize 2D heterostructure is a promising

route as it allows control over the sequence of the layers due to the electrostatic interactions and assembly processes in solution, such as chemical preintercalation synthesis.

Dopamine (DOPA) hydrochloride is a widely used carbon precursor because it can adhere to a wide range of organic and inorganic surfaces, and it can efficiently polymerize and carbonize during heat treatment processes.<sup>44</sup> DOPA is also highly soluble in water which makes it an attractive carbon precursor to incorporate into an aqueous-based synthesis approach.

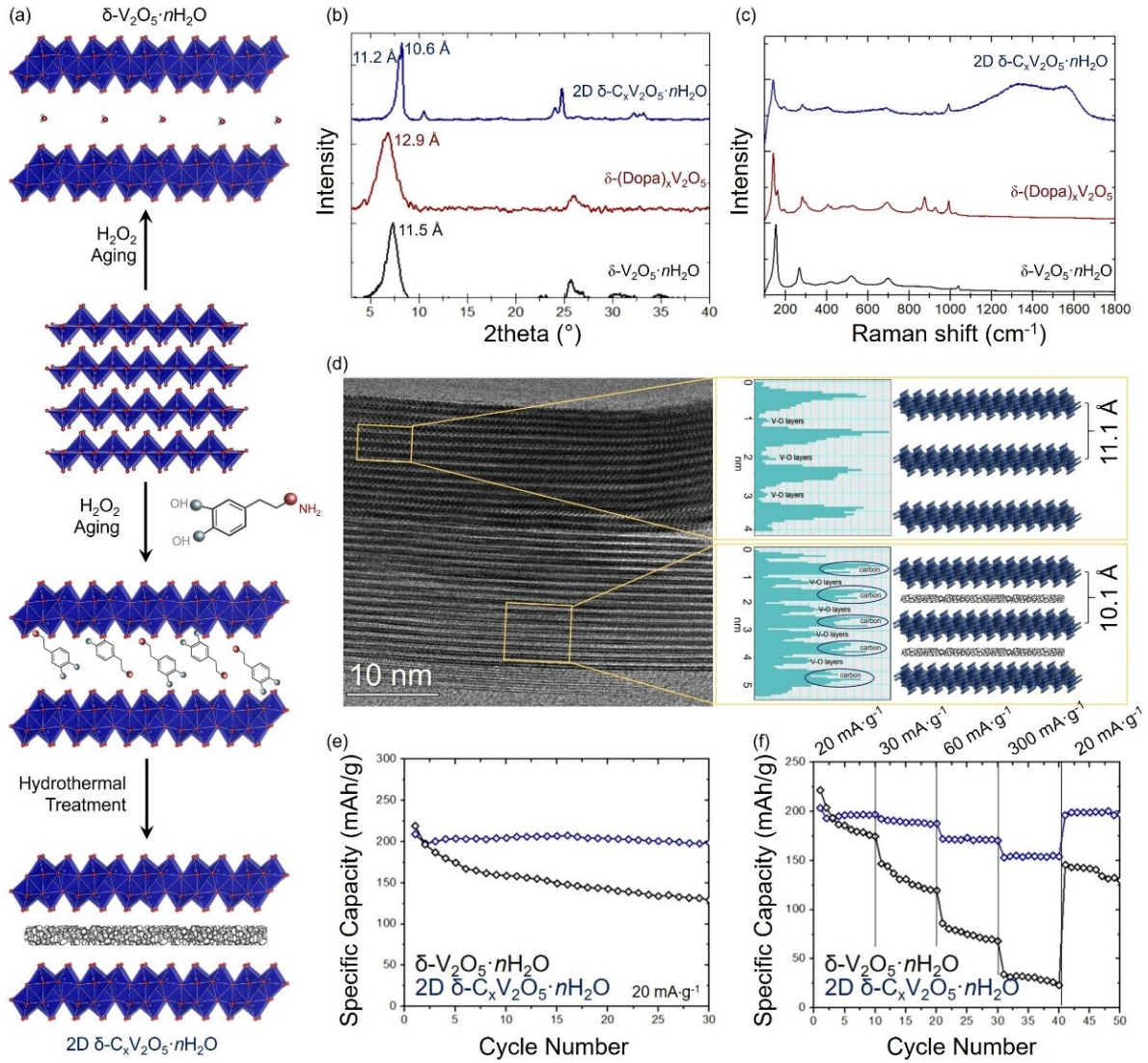


**Figure 8.** Formation of the oxide-carbon heterointerface via chemical preintercalation synthesis. (a) Schematic illustration of the synthesis strategy for the preparation of 2D  $\delta$ - $\text{C}_x\text{V}_2\text{O}_5\cdot n\text{H}_2\text{O}$  heterostructure and reference  $\delta\text{-V}_2\text{O}_5\cdot n\text{H}_2\text{O}$  material. (b) XRD patterns and (c) Raman spectra of the  $\delta\text{-(Dopa)}_x\text{V}_2\text{O}_5$  precursor,  $\delta\text{-C}_x\text{V}_2\text{O}_5\cdot n\text{H}_2\text{O}$  and  $\delta\text{-V}_2\text{O}_5\cdot n\text{H}_2\text{O}$  materials. (d) BF-STEM image of a  $\delta\text{-V}_2\text{O}_5\cdot n\text{H}_2\text{O}$  nanobelt (top) and 2D  $\delta$ - $\text{C}_x\text{V}_2\text{O}_5\cdot n\text{H}_2\text{O}$  nanobelt (bottom) combined with the averaged line histograms extracted by analyzing contrast in rectangular areas outlined in yellow in BF-STEM image. (e, f) Electrochemical cycling properties of non-aqueous Li-ion cells containing 2D  $\delta$ - $\text{C}_x\text{V}_2\text{O}_5\cdot n\text{H}_2\text{O}$  heterostructure and  $\delta\text{-V}_2\text{O}_5\cdot n\text{H}_2\text{O}$  electrodes. (e) Cycling stability at a current density of 20 mA/g. (f) Rate capability at increasing current densities shown in the figure. Adapted with permission from ref. 4. Copyright 2020 American Chemical Society.

Motivated by their properties, we utilized chemical preintercalation of DOPA molecules between bilayers of vanadium oxide followed by the hydrothermal treatment, leading to carbonization of organic molecules, to form a layered  $\delta\text{-C}_x\text{V}_2\text{O}_5\cdot n\text{H}_2\text{O}$  heterostructure (**Figure 8a**).<sup>4</sup> We found that chemical preintercalation of dopamine led to increase in the interlayer spacing, which has then decreased after hydrothermal treatment of the dopamine-preintercalated BVO intermediate phase (**Figure 8b**). The (001) peak in the XRD pattern of 2D heterostructure showed clear splitting into two peaks that correspond to interlayer spacings of 11.2 and 10.6 Å. Raman spectra revealed the presence of highly disordered carbon layers in 2D heterostructure (**Figure 8c**). The presence of carbon layers was further confirmed by scanning transmission electron microscopy (**Figure 8d**). A line of light grey was observed in the middle of the interlayer regions, which suggested the presence of a carbon layer. This feature was further highlighted in the line-averaged histogram extracted from the selected regions. For some parts of the nanobelt, the line-averaged histogram showed only deep dips in contrast intensity, which correspond to the vanadium oxide layers. However, in other nanobelt areas, the vanadium oxide bilayers are marked by the deepest dips in intensity, were accompanied by additional dips in the dark, high intensity interlayer regions, which provided direct evidence for the presence of carbon layers. We have also confirmed the formation of the carbon layer by electronic conductivity measurements: the electronic conductivity of the 2D heterostructure phase was found to be two orders of magnitude higher than that of the pristine BVO.

We studied the electrochemical performance of the pristine BVO and the 2D heterostructure electrodes was studied in Li-ion cells (**Figure 8e, 8f**). At a current density of 20 mA g<sup>-1</sup>, BVO electrodes showed an initial discharge capacity of 219 mAh·g<sup>-1</sup>, which quickly decayed over extended cycling, exhibiting a capacity retention of 58% after 30 discharge/charge cycles. While

the 2D heterostructure electrodes demonstrated a slightly lower initial discharge capacity of 206  $\text{mAh}\cdot\text{g}^{-1}$ , they exhibited significantly higher capacity retention compared to the reference material, with 94% of the initial capacity retained after 30 cycles. We attributed the improved capacity retention to the formation of robust heterointerfaces between the carbon and vanadium oxide layers, which stabilized the lamellar ordering of the layers and led to enhanced structural and therefore electrochemical stability. The rate capability evaluated by cycling Li-ion cells at various current densities clearly showed that the electrode material containing carbon layers exhibited significantly higher capacities at increased current densities. Such electrochemical behavior indicates improved charge transport kinetics, leading to improved tolerance of high currents. The increase in rate capability of the heterostructure electrodes can be ascribed to the improved electron transport via the carbon layers accommodated between vanadium oxide layers combined with the presence of 2D diffusion channels available for the electrochemically cycled  $\text{Li}^+$  ion movement. The presence of the carbon layer in the interlayer region of BVO is likely to affect diffusion of electrochemically cycled ions, especially in case of defect-rich amorphous carbon. In this work, however, the carbon layers formed intermittently, and carbon-free areas in the interlayer region enabled efficient transport of  $\text{Li}^+$  ions. Enrichment of the produced materials with carbon could be achieved by increasing concentration of organic molecular ions in chemical preintercalation synthesis process, which can however lead to phase separation and formation of nanocomposites.<sup>45</sup> More studies are required to understand the mechanism of transformation to controllably synthesize materials with oxide/carbon heterointerfaces.

## CONCLUSIONS AND OUTLOOK

The examples discussed in this Account demonstrate that the chemical preintercalation synthesis approach allows atomic-level control for the preparation of new materials with targeted structures

and tunable electrochemical charge storage properties. We showed how by selecting precursors in the reacting mixture, the interlayer chemistry, interlayer distance, and morphology of the produced layered phases can be controlled, and how these parameters enable tunability of ion diffusion, electronic conductivity, and structural stability of these materials when they used as electrodes in reversible reactions of interactions with ions from electrolytes. We believe that more substantial advances in energy storage technology can be achieved via chemical preintercalation synthesis of electrode materials. Some progress has been already reported,<sup>46</sup> however with the growing family of chemically preintercalated materials new insights are forthcoming. In the following paragraphs, we discuss the prospects of chemical preintercalation for future developments.

Hydrated layered ion preintercalated phases showed promise in improving charge storage capacity and electrochemical stability, however, the hydration degree and interlayer ion content are often fixed parameters. Computationally guided experiments can help understand how the amount of confined ions and water will affect charge storage properties, expansion/contraction of the interlayer region and associated stresses and strains. The variation of chemical composition of the confined interlayer region needs to be combined with the experimentally measured diffusion coefficients and computational predictions of the ion diffusion and structure stability, including diffusion energy barriers and ion diffusion pathways depending on the nature of chemically preintercalated and electrochemically cycled ions. Chemical preintercalation of  $\text{Al}^{3+}$  ion into the interlayer spacing of the oxide structure remained unsuccessful at the time of this account publication. Inserting  $\text{Al}^{3+}$  ion can be beneficial not only for the synthesis of new cathode materials for Al-ion batteries, but it also can allow increasing the interlayer distance beyond that obtained with chemical preintercalation of  $\text{Mg}^{2+}$  ion and demonstrate energy storage properties superior to those achieved by Mg-preintercalated BVO. The radius of the hydrated  $\text{Al}^{3+}$  ion is 4.75 Å (for

comparison, the radius of the hydrated  $Mg^{2+}$  ion is 4.28 Å), which can lead to the chemically preintercalated layered oxides with the record large interlayer distance obtained with inorganic ions. Better control of the chemistry of the layers can further improve charge storage properties of chemically preintercalated materials. The control of transition metal ion in the composition of the structural layer can enable further tunability of charge storage properties, including potentials, specific capacities, stability, electronic conductivity and rate capability. This can be achieved, for example, by using precursors of different transition metal ions in the synthesis or by utilizing solid solution MXene precursors. Moreover, it is important to analyze the interactions between pillaring species and host structure as well as the expansion/contraction of the pillared phases during electrochemical cycling, requiring joint efforts from the experimentalists and theorists. Some insights could be obtained through *in situ* XRD<sup>29</sup> and operando atomic force microscopy<sup>47</sup> experiments. *In situ* monitoring of the interlayer water is necessary to fully understand its dynamics and how it affects evolution of the components in the system during cycling. Such experiments are challenging as they require monitoring of not so easily detectable species and a cell as a whole, which could be achieved by the multidisciplinary team of scientists. Phase evolution of the chemically preintercalated layered phases at gradually increased temperatures needs further investigation to understand the temperature stability window for each of the metastable ion preintercalated oxides. Additionally, chemically preintercalated phases with open layered crystal structure can serve as precursor to obtain more crystallographically dense complex oxides via annealing at high temperatures. Understanding temperature-induced phase evolution as a function of ionic content can enable controllable synthesis of new functional materials.

With organic molecules, it remains unclear how versatile the chemical preintercalation synthesis approach can be when the nature of the organic ion is changes. For example, chemical

preintercalation of the redox active organic ions can be used to enhance charge storage properties of the synthesized materials via combined redox processes associated with transition metal ion in the structural layer and organic molecules in the interlayer region. In order to synthesize such new hybrid phases, it is necessary to understand how the chemical composition of organic molecules affects chemical preintercalation processes. The role of hydroxyl, amine, and aromatic groups needs to be unveiled. While carbonization of chemically preintercalated dopamine molecules was shown to lead to improved electrochemical stability and rate capability, it is still unclear how efficient carbonization of organics can be promoted with the goal of obtaining graphitic rather than amorphous carbon, and extended carbon layers rather than small islands.

*In situ* investigation of the chemically preintercalated oxides with expanded interlayer regions can shed light on volumetric characteristics of charge storage properties. In fact, expanded interlayer regions assume low volumetric capacity, however only under the assumption that one row of electrochemically cycled ions intercalates into the interlayer region. However, with expanded layers, two or more layers of electrochemically cycled ions can reside in the interlayer region. Such phenomenon has been demonstrated for MXene electrodes cycled ion Na-ion cells.<sup>48</sup> No experimental data exists on the analysis of the atomic structure of discharged chemically preintercalated oxides. We need to better understand the mechanism of charge storage and *in situ* structure evolution of chemically preintercalated electrodes in energy storage devices.

Due to the well-established sol-gel and precipitation chemistries of transition metal oxides, synthesis of versatile chemically preintercalated materials is possible and new reports are expected on the synthesis of new materials. In addition, other synthetic approaches, such as ion exchange reactions<sup>49</sup> and post-exfoliation chemical preintercalation reactions in solutions,<sup>50</sup> can be used. As a result of these research efforts, materials synthesized via the chemical preintercalation approach

can advance energy storage technology by offering improved ion storage capacities, controllable potentials, extended electrochemical stability and higher tolerance towards high currents.

## **AUTHOR INFORMATION**

### **Corresponding Author**

\*E-mail: [ep423@drexel.edu](mailto:ep423@drexel.edu)

### **ORCID**

Ekaterina Pomerantseva: 0000-0002-6765-7133

### **Notes**

The author declares no competing financial interest.

### **Biography**

Ekaterina Pomerantseva is an Associate Professor in the Department of Materials Science and Engineering at Drexel University. She is leading a research group studying how structure and properties of materials can be controlled via rational design of the synthesis pathways with a focus on electrochemical applications.

## **ACKNOWLEDGEMENTS**

The author acknowledges the National Science Foundation Grant Nos. DMR-1609272, DMR-1752623 and DMR-2106445 and the Center for Mesoscale Transport Properties, an Energy Frontier Research Center supported by the U.S. Department of Energy, Office of Science, Basic Energy Sciences, under award #DE-SC0012673 for financial support.

## REFERENCES

- (1) Clites, M.; Hart, J. L.; Taheri, M. L.; Pomerantseva, E. Chemically Preintercalated Bilayered  $K_xV_2O_5 \cdot nH_2O$  Nanobelts as a High-Performing Cathode Material for K-Ion Batteries. *ACS Energy Letters* **2018**, 3 (3), 562-567. DOI: 10.1021/acsenergylett.7b01278.
- (2) Clites, M.; Pomerantseva, E. Bilayered vanadium oxides by chemical pre-intercalation of alkali and alkali-earth ions as battery electrodes. *Energy Storage Materials* **2018**, 11, 30-37. DOI: <https://doi.org/10.1016/j.ensm.2017.09.005>.
- (3) Ridley, P.; Gallano, C.; Andris, R.; Shuck, C. E.; Gogotsi, Y.; Pomerantseva, E. MXene-Derived Bilayered Vanadium Oxides with Enhanced Stability in Li-Ion Batteries. *ACS Applied Energy Materials* **2020**, 3 (11), 10892–10901. DOI: 10.1021/acsaem.0c01906.
- (4) Clites, M.; Andris, R.; Cullen, D. A.; More, K. L.; Pomerantseva, E. Improving Electronic Conductivity of Layered Oxides through the Formation of Two-Dimensional Heterointerface for Intercalation Batteries. *ACS Applied Energy Materials* **2020**, 3 (4), 3835-3844. DOI: 10.1021/acsaem.0c00274.
- (5) Li, M.; Lu, J.; Chen, Z. W.; Amine, K. 30 Years of Lithium-Ion Batteries. *Advanced Materials* **2018**, 30 (33), 1800561. DOI: 10.1002/adma.201800561.
- (6) Tian, Y. S.; Zeng, G. B.; Rutt, A.; Shi, T.; Kim, H.; Wang, J. Y.; Koettgen, J.; Sun, Y. Z.; Ouyang, B.; Chen, T. N.; et al. Promises and Challenges of Next-Generation "Beyond Li-ion" Batteries for Electric Vehicles and Grid Decarbonization. *Chemical Reviews* **2021**, 121 (3), 1623-1669. DOI: 10.1021/acs.chemrev.0c00767.
- (7) Peng, L. L.; Zhu, Y.; Chen, D. H.; Ruoff, R. S.; Yu, G. H. Two-Dimensional Materials for Beyond-Lithium-Ion Batteries. *Advanced Energy Materials* **2016**, 6 (11), 1600025. DOI: 10.1002/aenm.201600025.
- (8) Suo, L. M.; Borodin, O.; Gao, T.; Olguin, M.; Ho, J.; Fan, X. L.; Luo, C.; Wang, C. S.; Xu, K. "Water-in-salt" electrolyte enables high-voltage aqueous lithium-ion chemistries. *Science* **2015**, 350 (6263), 938-943. DOI: 10.1126/science.aab1595.
- (9) Whittingham, M. S. Lithium batteries and cathode materials. *Chemical Reviews* **2004**, 104 (10), 4271-4301. DOI: 10.1021/cr020731c.
- (10) Pomerantseva, E.; Gogotsi, Y. Two-dimensional heterostructures for energy storage. *Nature Energy* **2017**, 2 (7), 17089. DOI: 10.1038/nenergy.2017.89.
- (11) Nitta, N.; Wu, F.; Lee, J. T.; Yushin, G. Li-ion battery materials: present and future. *Materials Today* **2015**, 18 (5), 252-264. DOI: <https://doi.org/10.1016/j.mattod.2014.10.040>.
- (12) Livage, J.; Henry, M.; Sanchez, C. Sol-gel chemistry of transition metal oxides. *Progress in Solid State Chemistry* **1988**, 18 (4), 259-341. DOI: [https://doi.org/10.1016/0079-6786\(88\)90005-2](https://doi.org/10.1016/0079-6786(88)90005-2).
- (13) Clites, M.; Pomerantseva, E. *Synthesis of hybrid layered electrode materials via chemical pre-intercalation of linear organic molecules*; SPIE, 2018.
- (14) Clites, M.; Byles, B. W.; Pomerantseva, E. Effect of aging and hydrothermal treatment on electrochemical performance of chemically pre-intercalated Na–V–O nanowires for Na-ion

batteries. *Journal of Materials Chemistry A* **2016**, *4* (20), 7754-7761, 10.1039/C6TA02917E. DOI: 10.1039/C6TA02917E.

(15) Clites, M.; Hart, J. L.; Taheri, M. L.; Pomerantseva, E. Annealing-Assisted Enhancement of Electrochemical Stability of Na-Preintercalated Bilayered Vanadium Oxide Electrodes in Na-Ion Batteries. *ACS Applied Energy Materials* **2020**, *3* (1), 1063-1075. DOI: 10.1021/acsaem.9b02098.

(16) Mai, L. Q.; Hu, B.; Chen, W.; Qi, Y. Y.; Lao, C. S.; Yang, R. S.; Dai, Y.; Wang, Z. L. Lithiated  $\text{MoO}_3$  Nanobelts with Greatly Improved Performance for Lithium Batteries. *Advanced Materials* **2007**, *19* (21), 3712-3716. DOI: <https://doi.org/10.1002/adma.200700883>. Mai, L.; Hu, B.; Qi, Y.; Dai, Y.; Chen, W. Improved Cycling Performance of Directly Lithiated  $\text{MoO}_3$  Nanobelts. *International Journal of Electrochemical Science* **2008**, *3*, 216-222.

(17) Dong, Y.; Xu, X.; Li, S.; Han, C.; Zhao, K.; Zhang, L.; Niu, C.; Huang, Z.; Mai, L. Inhibiting effect of  $\text{Na}^+$  pre-intercalation in  $\text{MoO}_3$  nanobelts with enhanced electrochemical performance. *Nano Energy* **2015**, *15*, 145-152. DOI: <https://doi.org/10.1016/j.nanoen.2015.04.015>.

(18) Petkov, V.; Trikalitis, P. N.; Bozin, E. S.; Billinge, S. J. L.; Vogt, T.; Kanatzidis, M. G. Structure of  $\text{V}_2\text{O}_5 \cdot n\text{H}_2\text{O}$  Xerogel Solved by the Atomic Pair Distribution Function Technique. *Journal of the American Chemical Society* **2002**, *124* (34), 10157-10162. DOI: 10.1021/ja026143y.

(19) Yao, J. H.; Li, Y. W.; Masse, R. C.; Uchaker, E.; Cao, G. Z. Revitalized interest in vanadium pentoxide as cathode material for lithium-ion batteries and beyond. *Energy Storage Materials* **2018**, *11*, 205-259. DOI: 10.1016/j.ensm.2017.10.014.

(20) Boyd, S.; Ganeshan, K.; Tsai, W.-Y.; Wu, T.; Saeed, S.; Jiang, D.-e.; Balke, N.; van Duin, A. C. T.; Augustyn, V. Effects of interlayer confinement and hydration on capacitive charge storage in birnessite. *Nature Materials* **2021**, *20* (12), 1689-1694. DOI: 10.1038/s41563-021-01066-4.

(21) Yin, J.; Pelliccione, C. J.; Lee, S. H.; Takeuchi, E. S.; Takeuchi, K. J.; Marschilok, A. C. Communication—Sol-Gel Synthesized Magnesium Vanadium Oxide,  $\text{Mg}_x\text{V}_2\text{O}_5 \cdot n\text{H}_2\text{O}$ : The Role of Structural  $\text{Mg}^{2+}$ on Battery Performance. *Journal of The Electrochemical Society* **2016**, *163* (9), A1941-A1943. DOI: 10.1149/2.0781609jes.

(22) Kundu, D.; Adams, B. D.; Duffort, V.; Vajargah, S. H.; Nazar, L. F. A high-capacity and long-life aqueous rechargeable zinc battery using a metal oxide intercalation cathode. *Nature Energy* **2016**, *1* (10), 16119. DOI: 10.1038/nenergy.2016.119.

(23) Clites, M.; Pomerantseva, E. *The ion dependent change in the mechanism of charge storage of chemically preintercalated bilayered vanadium oxide electrodes*; SPIE, 2017.

(24) Wang, J.; Polleux, J.; Lim, J.; Dunn, B. Pseudocapacitive Contributions to Electrochemical Energy Storage in  $\text{TiO}_2$  (Anatase) Nanoparticles. *The Journal of Physical Chemistry C* **2007**, *111* (40), 14925-14931. DOI: 10.1021/jp074464w.

(25) Wei, Q.; Jiang, Z.; Tan, S.; Li, Q.; Huang, L.; Yan, M.; Zhou, L.; An, Q.; Mai, L. Lattice Breathing Inhibited Layered Vanadium Oxide Ultrathin Nanobelts for Enhanced Sodium Storage. *ACS Applied Materials & Interfaces* **2015**, *7* (33), 18211-18217. DOI: 10.1021/acsami.5b06154.

(26) Moretti, A.; Giuli, G.; Trapananti, A.; Passerini, S. Electrochemical and structural investigation of transition metal doped  $\text{V}_2\text{O}_5$  sono-aerogel cathodes for lithium metal batteries. *Solid State Ionics* **2018**, *319*, 46-52. DOI: <https://doi.org/10.1016/j.ssi.2018.01.040>.

(27) Tepavcevic, S.; Xiong, H.; Stamenkovic, V. R.; Zuo, X.; Balasubramanian, M.; Prakapenka, V. B.; Johnson, C. S.; Rajh, T. Nanostructured Bilayered Vanadium Oxide Electrodes for Rechargeable Sodium-Ion Batteries. *ACS Nano* **2012**, *6* (1), 530-538. DOI: 10.1021/nn203869a.

(28) Mukherjee, S.; Quilty, C. D.; Yao, S.; Stackhouse, C. A.; Wang, L.; Takeuchi, K. J.; Takeuchi, E. S.; Wang, F.; Marschilok, A. C.; Pomerantseva, E. The effect of chemically preintercalated alkali ions on the structure of layered titanates and their electrochemistry in aqueous energy storage systems. *Journal of Materials Chemistry A* **2020**, *8* (35), 18220-18231, 10.1039/D0TA04545D. DOI: 10.1039/D0TA04545D.

(29) Liu, L.; Wu, Y.-C.; Huang, L.; Liu, K.; Dupoyer, B.; Rozier, P.; Taberna, P.-L.; Simon, P. Alkali Ions Pre-Intercalated Layered MnO<sub>2</sub> Nanosheet for Zinc-Ions Storage. *Advanced Energy Materials* **2021**, *11* (31), 2101287. DOI: <https://doi.org/10.1002/aenm.202101287>.

(30) Rahman, A. U.; Zarshad, N.; Jianghua, W.; Shah, M.; Ullah, S.; Li, G.; Tariq, M.; Ali, A. Sodium Pre-Intercalation-Based Na<sub>3</sub>-δ-MnO<sub>2</sub>@CC for High-Performance Aqueous Asymmetric Supercapacitor: Joint Experimental and DFT Study. *Nanomaterials* **2022**, *12* (16), 2856.

(31) Clites, M.; Blickley, A.; Cullen, D. A.; Pomerantseva, E. Chemical Preintercalation Synthesis Approach for the Formation of New Layered Tungsten Oxides. *Journal of Materials Science* **2022**, *57*, 7814–7826.

(32) Wangoh, L. W.; Huang, Y.; Jezorek, R. L.; Kehoe, A. B.; Watson, G. W.; Omenya, F.; Quackenbush, N. F.; Chernova, N. A.; Whittingham, M. S.; Piper, L. F. J. Correlating Lithium Hydroxyl Accumulation with Capacity Retention in V<sub>2</sub>O<sub>5</sub> Aerogel Cathodes. *ACS Applied Materials & Interfaces* **2016**, *8* (18), 11532-11538. DOI: 10.1021/acsami.6b02759.

(33) Mitchell, J. B.; Geise, N. R.; Paterson, A. R.; Osti, N. C.; Sun, Y.; Fleischmann, S.; Zhang, R.; Madsen, L. A.; Toney, M. F.; Jiang, D.-e.; et al. Confined Interlayer Water Promotes Structural Stability for High-Rate Electrochemical Proton Intercalation in Tungsten Oxide Hydrates. *ACS Energy Letters* **2019**, *4* (12), 2805-2812. DOI: 10.1021/acsenergylett.9b02040. Mitchell, J. B.; Lo, W. C.; Genc, A.; LeBeau, J.; Augustyn, V. Transition from Battery to Pseudocapacitor Behavior via Structural Water in Tungsten Oxide. *Chemistry of Materials* **2017**, *29* (9), 3928-3937. DOI: 10.1021/acs.chemmater.6b05485.

(34) Charles, D. S.; Feygenson, M.; Page, K.; Neufeld, J.; Xu, W.; Teng, X. Structural water engaged disordered vanadium oxide nanosheets for high capacity aqueous potassium-ion storage. *Nature Communications* **2017**, *8* (1), 15520. DOI: 10.1038/ncomms15520.

(35) Shan, X.; Guo, F.; Charles, D. S.; Lebens-Higgins, Z.; Abdel Razek, S.; Wu, J.; Xu, W.; Yang, W.; Page, K. L.; Neufeld, J. C.; et al. Structural water and disordered structure promote aqueous sodium-ion energy storage in sodium-birnessite. *Nature Communications* **2019**, *10* (1), 4975. DOI: 10.1038/s41467-019-12939-3.

(36) Naguib, M.; Kurtoglu, M.; Presser, V.; Lu, J.; Niu, J.; Heon, M.; Hultman, L.; Gogotsi, Y.; Barsoum, M. W. Two-Dimensional Nanocrystals Produced by Exfoliation of Ti<sub>3</sub>AlC<sub>2</sub>. *Advanced Materials* **2011**, *23* (37), 4248-4253. DOI: <https://doi.org/10.1002/adma.201102306>. Naguib, M.; Barsoum, M. W.; Gogotsi, Y. Ten Years of Progress in the Synthesis and Development of MXenes. *Advanced Materials* **2021**, *33* (39), 2103393. DOI: <https://doi.org/10.1002/adma.202103393>.

(37) Dong, Y.; Wu, Z.-S.; Zheng, S.; Wang, X.; Qin, J.; Wang, S.; Shi, X.; Bao, X. Ti<sub>3</sub>C<sub>2</sub> MXene-Derived Sodium/Potassium Titanate Nanoribbons for High-Performance Sodium/Potassium Ion

Batteries with Enhanced Capacities. *ACS Nano* **2017**, *11* (5), 4792-4800. DOI: 10.1021/acsnano.7b01165.

(38) Wu, H.; Almalki, M.; Xu, X.; Lei, Y.; Ming, F.; Mallick, A.; Roddatis, V.; Lopatin, S.; Shekhah, O.; Eddaoudi, M.; et al. MXene Derived Metal–Organic Frameworks. *Journal of the American Chemical Society* **2019**, *141* (51), 20037-20042. DOI: 10.1021/jacs.9b11446.

(39) Kanatzidis, M. G.; Wu, C. G.; Marcy, H. O.; DeGroot, D. C.; Kannewurf, C. R. Conductive polymer/oxide bronze nanocomposites. Intercalated polythiophene in vanadium pentoxide ( $V_2O_5$ ) xerogels. *Chemistry of Materials* **1990**, *2* (3), 222-224. DOI: 10.1021/cm00009a005. Kanatzidis, M. G.; Wu, C. G.; Marcy, H. O.; Kannewurf, C. R. Conductive-polymer bronzes. Intercalated polyaniline in vanadium oxide xerogels. *Journal of the American Chemical Society* **1989**, *111* (11), 4139-4141. DOI: 10.1021/ja00193a078.

(40) Yucesan, G.; Golub, V.; O'Connor, C. J.; Zubieta, J. Solid state coordination chemistry: organic/inorganic hybrid frameworks constructed from tetrapyridylporphyrin and vanadium oxide chains. *CrystEngComm* **2004**, *6* (57), 323-325, 10.1039/B414430A. DOI: 10.1039/B414430A.

(41) Quites, F. J.; Bisio, C.; Vinhas, R. C. G.; Landers, R.; Marchese, L.; Pastore, H. d. O. Vanadium oxide intercalated with polyelectrolytes: novel layered hybrids with anion exchange properties. *Journal of colloid and interface science* **2012**, *368* 1, 462-469.

(42) Liu, W.; Wang, Z.; Su, Y.; Li, Q.; Zhao, Z.; Geng, F. Molecularly Stacking Manganese Dioxide/Titanium Carbide Sheets to Produce Highly Flexible and Conductive Film Electrodes with Improved Pseudocapacitive Performances. *Advanced Energy Materials* **2017**, *7* (22), 1602834. DOI: <https://doi.org/10.1002/aenm.201602834>.

(43) Pan, Q.; Zhang, Q.; Zheng, F.; Liu, Y.; Li, Y.; Ou, X.; Xiong, X.; Yang, C.; Liu, M. Construction of  $MoS_2/C$  Hierarchical Tubular Heterostructures for High-Performance Sodium Ion Batteries. *ACS Nano* **2018**, *12* (12), 12578-12586. DOI: 10.1021/acsnano.8b07172.

(44) Lee, H.; Dellatore, S. M.; Miller, W. M.; Messersmith, P. B. Mussel-Inspired Surface Chemistry for Multifunctional Coatings. *Science* **2007**, *318* (5849), 426-430. DOI: doi:10.1126/science.1147241.

(45) Norouzi, N.; Averianov, T.; Kuang, J.; Bock, D. C.; Yan, S.; Wang, L.; Takeuchi, K. J.; Takeuchi, E. S.; Marschilok, A. C.; Pomerantseva, E. Hierarchically structured  $MoO_2$ /dopamine-derived carbon spheres as intercalation electrodes for lithium-ion batteries. *Materials Today Chemistry* **2022**, *24*, 100783. DOI: <https://doi.org/10.1016/j.mtchem.2022.100783>.

(46) Yao, X.; Zhao, Y.; Castro, F. A.; Mai, L. Rational Design of Preintercalated Electrodes for Rechargeable Batteries. *ACS Energy Letters* **2019**, *4* (3), 771-778. DOI: 10.1021/acsenergylett.8b02555. Liu, Z.; Sun, H.; Qin, L.; Cao, X.; Zhou, J.; Pan, A.; Fang, G.; Liang, S. Interlayer Doping in Layered Vanadium Oxides for Low-cost Energy Storage: Sodium-ion Batteries and Aqueous Zinc-ion Batteries. *ChemNanoMat* **2020**, *6* (11), 1553-1566. DOI: <https://doi.org/10.1002/cnma.202000384>.

(47) Tsai, W.-Y.; Wang, R.; Boyd, S.; Augustyn, V.; Balke, N. Probing local electrochemistry via mechanical cyclic voltammetry curves. *Nano Energy* **2021**, *81*, 105592. DOI: <https://doi.org/10.1016/j.nanoen.2020.105592>.

(48) Wang, X.; Shen, X.; Gao, Y.; Wang, Z.; Yu, R.; Chen, L. Atomic-Scale Recognition of Surface Structure and Intercalation Mechanism of  $Ti_3C_2X$ . *Journal of the American Chemical Society* **2015**, *137* (7), 2715-2721. DOI: 10.1021/ja512820k.

(49) Fleischmann, S.; Sun, Y.; Osti, N. C.; Wang, R.; Mamontov, E.; Jiang, D.-e.; Augustyn, V. Interlayer separation in hydrogen titanates enables electrochemical proton intercalation. *Journal of Materials Chemistry A* **2020**, *8* (1), 412-421, 10.1039/C9TA11098D. DOI: 10.1039/C9TA11098D.

(50) Brady, A.; Liang, K.; Vuong, V. Q.; Sacci, R.; Prenger, K.; Thompson, M.; Matsumoto, R.; Cummings, P.; Irle, S.; Wang, H.-W.; et al. Pre-Sodiated  $Ti_3C_2T_x$  MXene Structure and Behavior as Electrode for Sodium-Ion Capacitors. *ACS Nano* **2021**, *15* (2), 2994-3003. DOI: 10.1021/acsnano.0c09301.